# Phenotypic continuum and poor intracytoplasmic sperm injection intracytoplasmic sperm injection prognosis in patients harboring HENMT1 variants

Zeina Wehbe, Anne-laure Barbotin, Angèle Boursier, Caroline Cazin, Jean-pascal Hograindleur, Marie Bidart, Emeline Fontaine, Pauline Plouvier, Florence Puch, Véronique Satre, et al.

# Full title: Phenotypic Continuum and Poor ICSI Prognosis in patients harboring *HENMT1* variants

**Short title:** Phenotypic continuum of *HENMT1* variants

**Authors:** Zeina Wehbe[1,2,†], Anne-Laure Barbotin[3,†], Angèle Boursier[3], Caroline Cazin[1,4], Jean-Pascal Hograindleur[5], Marie Bidart[1,6], Emeline Fontaine[1], Pauline Plouvier[7], Florence Puch[8], Véronique Satre[1,2], Christophe Arnoult[1], Selima Fourati Ben Mustapha[9], Raoudha Zouari[9], Nicolas Thierry-Mieg[10], Pierre F. Ray[1,4], Zine-Eddine Kherraf[1,4], Charles Coutton[1,2,‡,*], Guillaume Martinez[1,2,‡,*]

1. Université Grenoble Alpes, CNRS UMR 5309, INSERM U1209, Institute for Advanced Biosciences (IAB), Site Santé – Allée des Alpes, 38700 La Tronche, France

2. CHU Grenoble Alpes, Hôpital Couple-Enfant, UM de Génétique Chromosomique, 38000 Grenoble, France

3. CHU Lille, Institut de Biologie de la Reproduction-Spermiologie-CECOS, 59000 Lille, France

4. CHU Grenoble Alpes, UM GI-DPI, 38000 Grenoble, France

5. CHU Grenoble Alpes, UF de Biologie de la Procréation, 38000, Grenoble, France

6. CHU Grenoble Alpes, Laboratoire de Génétique Moléculaire: Maladies Héréditaires et Oncologie, 38000 Grenoble, France

7. CHU Lille, Service d'Assistance Médicale à la Procréation et Préservation de la Fertilité, 59000 Lille, France

8. CHU Grenoble Alpes, Laboratoire de Biochimie et Génétique Moléculaire, 38000 Grenoble, France

9. Centre d'Aide Médicale à la Procréation, Polyclinique les Jasmin, Centre Urbain Nord, Tunis 1003, Tunisia

10. Université Grenoble Alpes, CNRS, TIMC-IMAG, 38000 Grenoble, France

† Z.W. and A-L.B. should be regarded as first authors respectively

‡ C.C. and G.M. should be regarded as last authors respectively

*corresponding authors: gmartinez@chu-grenoble.fr ; ccoutton@chu-grenoble.fr

ORCID iDs: Guillaume Martinez http://orcid.org/0000-0002-7572-9096 ; Charles Coutton http://orcid.org/0000-0002-8873-8098

Other authors email address: zwehbe@chu-grenoble.fr (Z.W.), Annelaure.BARBOTIN@chu-lille.fr (A-L.B.), Angele.BOURSIER@chu-lille.fr (A.B.), Cazin.caroline@gmail.com (C.Ca.), JPHograindleur1@chu-grenoble.fr (J-P.H.), mbidart@chu-grenoble.fr (M.B.), emeline.fontaine@inserm.fr (E.F.), pauline.PLOUVIER@chu-lille.fr (P.P.), fpuch@chu-grenoble.fr (F.P.), vsatre@chu-grenoble.fr (V.S.), christophe.arnoult@univ-grenoble-alpes.fr (C.A.),

fourati_selima@yahoo.fr (S.F.B.M.), raouzou@gmail.com (R.Z.), Nicolas.Thierry-Mieg@univ-grenoble-alpes.fr (N.T-M.), pray@chu-grenoble.fr (P.F.R.), zkherraf@chu-grenoble.fr (Z.K.)

**Key words**

Infertility, piwi pathway, piRNA, spermatozoa, azoospermia, teratozoospermia

**Abstract**

Background: Small RNAs interacting with PIWI (piRNAs) play a crucial role in regulating transposable elements and translation during spermatogenesis and are essential in male germ cell development. Disruptions in the piRNA pathway typically lead to severe spermatogenic defects and thus male infertility. The *HENMT1* gene is a key player in piRNAs primary biogenesis and dysfunction of HENMT1 protein in meiotic and haploid germ cells resulted in the loss of piRNA methylation, piRNA instability, and TE de-repression. Henmt1-knockout mice exhibit a severe oligo-astheno-teratozoospermia (OAT) phenotype, whereas patients with *HENMT1* variants display more severe azoospermia phenotypes, ranging from meiotic arrest to hypospermatogenesis. Through whole-exome sequencing (WES) of infertile patient cohorts, we identified two new patients with variants in the *HENMT1* gene presenting spermatozoa in their ejcaulate, providing us the opportunity to study spermatozoa from these patients.

Objectives: Investigate the spermatozoa of two patients harboring a *HENMT1* variant to determine whether or not these scarce spermatozoa could be used with assisted reproductive technologies.

Materials and Methods: *HENMT1* variants identified by WES were validated through Sanger sequencing. Comprehensive semen analysis was conducted, and sperm cells were subjected to transmission electron microscopy for structural examination, *in situ* hybridization for aneuploidy assessment, and aniline blue staining for DNA compaction status. Subsequently, we assessed their suitability for *in vitro* fertilization using intracytoplasmic sperm injection (IVF-ICSI).

Results: Our investigations revealed a severe OAT phenotype similar to *knockout* mice, revealing altered sperm concentration, mobility, morphology, aneuploidy and nuclear compaction defects. Multiple IVF-ICSI attempts were also performed, but no live births were achieved.

Discussion: We confirm the crucial role of *HENMT1* in spermatogenesis and highlight a phenotypic continuum associated with *HENMT1* variants. Unfortunately, the clinical outcome of these genetic predispositions remains unfavourable, regardless of the patient's phenotype.

Conclusion: Presence of spermatozoa is insufficient to anticipate ICSI pregnancy success in *HENMT1* patients.

## INTRODUCTION

Infertility has emerged as a pressing global concern, impacting approximately 50 million couples worldwide who face challenges in natural reproduction despite 12 months of regular and unprotected intercourse[1]. This condition is clinically heterogeneous and characterized by a complex etiology. Consequently, despite its widespread prevalence, nearly 40% of infertile couples receive a diagnosis of unexplained or idiopathic infertility[2]. While acknowledging the multifaceted nature of infertility, it is crucial to recognize the significant role played by genetic defects in its manifestation. Studies suggest that up to half of idiopathic cases of male infertility may be linked to yet-to-be-identified genetic abnormalities[3]. Despite the diagnostic yield reaching up to 50% for certain rare phenotypes with known genetic causes[4], some severe form of male infertility like azoospermia, defined by the absence of sperm in the ejaculate, continues to present a diagnostic yield below 20%[5-6]. As researchers explore different transmission models[7] and treatment approaches[8], the identification of pathogenic variants within the genes associated with different molecular pathways in the testis remains of paramount importance for genetic and reproductive counselling, diagnostic precision, and potential future personalized medicine. Notably, the piRNA-pathway has gained considerable attention, and studies involving knockout mice and patients with bi-allelic variants in piRNA biogenesis-related genes consistently reveal severe disruptions in spermatogenesis, highlighting the pathway's critical role in male fertility (see[9-11] for review).

PIWI-interacting ribonucleic acids, or piRNAs, constitute a highly diverse class of small, single-stranded noncoding RNAs characterized by lengths ranging from 23 to 32 nucleotides. They bind to specific PIWI-clade members (from P-element Induced-WImpy testis) of the Argonaute protein family[12], and encompass over 8.5 million distinct sequences in human and 68.5 million in mouse[13]. According to their temporal expression patterns and sequence content, piRNAs are classified into fetal, pre-pachytene, and pachytene classes[14-15]. Fetal piRNAs are expressed in prospermatogonia and interact with PIWIL2 and PIWIL4[15]. Pre-pachytene piRNAs, detected in testes before germ cells enter the pachytene stage of meiotic prophase I, interact with PIWIL2 and are primarily involved in controlling the transposable elements[15-16]. Pachytene piRNAs, which are first produced when germ cells enter the pachytene stage of meiosis[15], account for approximately 95% of piRNAs in the adult testis[12], associate with PIWIL1 and PIWIL2[15], and are mainly involved in regulating post-meiotic gene expression[17-19].

Knockout mice for piRNA biogenesis-related genes predominantly exhibit a phenotype of non-obstructive azoospermia (NOA) characterized by germ cell maturation arrest at meiosis[20-25] or round spermatids stages[26-28]. In contrast, human patients present a more complex phenotypic continuum, ranging from Sertoli cells-only syndrome with absence of sperm production[11], through azoospermia due to meiotic arrest[29] or round spermatid arrest[30], to cryptozoospermia[31] and extreme and severe oligozoospermia[32-33] where spermatozoa are present in the ejaculate. This phenotypic continuum suggests that *in-vitro* fertilization with intracytoplasmic sperm injection (IVF-ICSI) could be an effective medical response for some of the patients, but it remains uncertain whether the few sperm cells produced are suitable for assisted medical procreation and compatible with a successful pregnancy[11,34].

The *HENMT1* gene, also known as Hen1 methyltransferase homolog 1, is a key player in piRNAs primary biogenesis, the pathway generating most of piRNAs in adult germ cells[35], where piRNas are processed from long non-coding RNAs transcribed from genomic piRNA clusters (see[12,36] for review). It encodes an enzyme responsible for catalyzing the 2'-O-methylation at the 3' end of piRNAs, a modification that contributes to their stability and functionality[37-39]. In line with the other essential genes involved in the piwi pathway, previous investigations revealed that dysfunction of HENMT1 protein in meiotic and haploid germ cells resulted in piRNA instability, the loss of piRNA methylation, and TE de-repression (in mice), leading to severe phenotype in both human[34] and mouse[37] models. *Henmt1*-knockout mice exhibit a severe oligo-astheno-teratozoospermia (OAT) phenotype characterized by a majority of pinhead sperm with stumpy tails lacking a mitochondrial sheath in the midpiece of the sperm tail[37]. In humans, three *HENMT1* variants were reported in three men displaying azoospermia of varying severity. Two patients harboring homozygote missense variants, c.226G>A;p.Gly76Arg and c.400A>T;p.Ile134Leu, respectively exhibited meiotic[34] and round spermatid arrest[11]. In contrast, a patient harboring a homozygous loss-of-function variant c.456C>G; p.Tyr152Ter exhibited hypospermatogenesis with positive testis sperm retrieval[34].

Through whole-exome sequencing of a cohort of azoospermic men, we previously identified[34] two of the cited patients (P0109_p.Gly76Arg and P0272_p.Tyr152Ter). Given the broad phenotypic continuum observed so far, we extended our search for variants to a cohort of teratozoospermic men. This strategy allowed us to identify two new patients with variants in the *HENMT1* gene: a novel biallelic loss-of-function variant c.100C>T;p.Gln34Ter and the already uncovered c.456C>G;p.Tyr152Ter variant. Spermatozoa were present in the ejaculate

of both patients, providing a unique opportunity to study them, characterize their nuclear quality, and assess their potential in IVF-ICSI.

## MATERIALS AND METHODS

### Patient recruitment

Patient P0582 and a fertile control were respectively recruited at the Hôpital Jeanne de Flandre - Lille University Hospital (France) and Grenoble-Alpes University Hospital (France). Patients P0109, P0272 and P1021 were recruited at the "Clinique des Jasmins" in Tunis (Tunisia). Informed consent was obtained from all individuals participating in the study according to local protocols and the principles of the Declaration of Helsinki. The study was approved by local ethics committees, and samples were then stored in the Centre de Resources Biologiques Germethèque (certification under ISO-9001 and NF-S 96–900) according to a standardized procedure, or were part of the Fertithèque collection declared to the French Ministry of Health (DC-2015–2580) and the French Data Protection Authority (DR-2016–392).

### Exome sequencing and bioinformatic analysis

Both entire cohort of respectively 245 azoospermic and 105 teratozoospermic patients underwent data processing following our established protocol[40]. Briefly, coding regions along with intron/exon boundaries were enriched using the Exon V6 kit from Agilent Technologies (Wokingham, UK), followed by sequencing on an Illumina HiSeq X platform by a contracted service provider (Novogene, Cambridge, UK). Exome data were analyzed using an in-house developed bioinformatics pipeline, comprising two modules available on GitHub under the GNU General Public License v3.0: https://github.com/ntm/grexome-TIMC-Primary and https://github.com/ntm/grexome-TIMC-Secondary, as previously detailed[41]. Variants with a minor allele frequency exceeding 1% in gnomAD v2.0 or 3% in the 1000 Genomes Project phase 3 were excluded, and only variants predicted to have high impact (e.g., stop-gain or frameshift variants) by the Variant Effect Predictor v110[42] were further examined.

### Sanger sequencing

The previous candidates and the newly identified *HENMT1* variants all underwent validation through Sanger sequencing conducted on an ABI 3500XL instrument (Applied Biosystems) and data analysis was conducted using SeqScape software (Applied Biosystems).

### Minigene splicing reporter assay

To further validate the deleterious impact of the previously identified c.226G>A;p.Gly76Arg variant and to better characterize its impact on RNA splicing, we performed a minigene assay.

DNAs from the proband patient, carrying the identified homozygous splicing variant of HENMT1 c.226G>A and DNA from a fertile control, WT for the variant c.226G, were amplified using a CloneAmp HiFi PCR Premix (#639298, Takara). Primers sequences (5'-3'), forward (intron 3): CCTACAGCGCACGCGTGAATGGGAAAACTGTGTGTACG and, reverse (intron 4): GTTGCTTTCCGTCGACATGGTTCAAAATGCAGGCGG (Figure S1A). The 1360 bp amplicon (c.151-335_263+356) was inserted between MluI and SalI restriction sites of the pCineo minigene vector as previously described[43], using ProLigation-Free Cloning Kit (#E086/E087, Abm) (Figure S1B). Constructed vectors were transformed in Escherichia coli DH5α- competent cells (#44-0097, Invitrogen) for amplification. DNA sequences of amplicons cloned into pCineo vector, WT and mutant plasmids were checked by DNA sequencing (3500xl Genetic Analyzer and SeqScape3 software, Thermo Fisher Scientific).

HEK 293T cells were purchased from the American Type Culture Collection (ATCC, USA) and grown in DMEM medium (#31966021) supplemented with 10% fetal bovine serum (#10270106), penicillin-streptomycin (respectively 100 U/L and 100mg/L, #15140122) all from ThermoFisherScientific. Cell cultures were incubated at 37°C and 5% CO2 in a humidified incubator. The day before transfection, 2.105 cells were plated in a 6-well culture plate and transiently transfected with 2µg of plasmids (empty pTB2 (control), pTB2- WT (WT) and pTB2- mutant) using calcium phosphate (#631312, Takara) according to the manufacturer's instructions. After 48h of incubation, cells were harvested with trypsin-EDTA (#15400054, ThermoFisherScientific) and total RNA was extracted (NucleoSpin RNA, #740955.50, Macherey Nagel). First-strand cDNA was synthesized from 1µg of extracted total RNA (SuperScript™ III First-Strand Synthesis SuperMix, #11752050, ThermoFisherScientific). The resulting cDNA was amplified by PCR using vector- specific primers surrounding the cloning site thank to CloneAmp HiFi PCR Premix (#639298, Takara). The PCR products were analyzed on 1% agarose gel. The target DNA bands were gel-cut, purified (PCR Clean up, #740609-250, Macherey Nagel) and sequenced to identify mutation impact on splicing process.

**Semen Analysis**

Semen samples were obtained by masturbation after three to four days of sexual abstinence and were incubated for 30 min at 37°C for liquefaction. Parameters evaluated according to World Health Organization (WHO) guidelines[44] were: ejaculate volume, pH and viscosity, and sperm cells concentration, vitality, motility and morphology.

**Transmission Electron Microscopy**

Transmission Electron Microscopy (TEM) experiments were performed like previously[45] using sperm cells from fertile control and patient P0582. After fixation in 2.0% v/v glutaraldehyde in phosphate buffer (pH 7.4), the sperm pellet underwent a 15 minutes wash in fresh buffer containing 4% w/v sucrose and was subsequently embedded in 2% agar. Post-fixation involved the use of 1% osmic acid in phosphate buffer. Following fixation, small pieces of agar containing spermatozoa were dehydrated through a graded series of ethanol. Subsequently, these pieces were further embedded in Epon resin (Polysciences Inc., Warrington, PA, USA). Sections were then cut using a Reichert OmU2 ultramicrotome (Reichert-Jung AG, Vienna, Austria) equipped with a diamond knife. Ultrathin sections (70 nm) were collected on Parlodion 0.8%/isoamyl acetate-coated 100 mesh Nickel grids (EMS, Fort Washington, PA, USA) and counterstained with 2% uranyl acetate and lead citrate before observation. Examination of the sections was conducted using a Zeiss transmission electron microscope 902 (Leo, Rueil-Malmaison, France), and images were acquired utilizing a Gatan Orius SC1000 CCD camera (Gatan France, Grandchamp, France).

**Immunostaining**

Immunofluorescence (IF) experiments were performed on fertile control and patient P0582. Sperm cells were fixed in phosphate-buffered saline (PBS) with 4% paraformaldehyde for 30 secondes at room temperature, washed two time in PBS and spotted onto 0.1% poly L-lysine pre-coated slides (Thermo Fisher Scientific,Waltham, MA, USA). After attachment, sperm were washed 2x5 minutes with 0.1% (v/v) Triton X-100-DPBS (Triton X-100; Sigma-Aldrich Co., Ltd., Irvine, UK) at room temerature. Slides were then blocked 30 minutes in 2% normal serum–0.1% (v/v) Triton X-100-DPBS (normal goat or donkey serum; GIBCO, Thermo Fisher Scientific) and incubated overnight at 4°C with the primary antibodies: polyclonal rabbit anti-HENMT1 (AB121991, Abcam (Cambridge, UK), 1:100) and monoclonal mouse anti-acetylated-β-tubulin (AB61601, Abcam (Cambridge, UK), 1:400). Washes were performed with 0.1% (v/v) Tween 20–DPBS, followed by 1 h incubation at room temperature with secondary antibodies (Dylight 488 and Dylight 549, Jackson Immunoresearch®, 1:1000) and counterstained with 5 mg/mL Hoechst 33342 (Sigma-Aldrich). Appropriate controls without primary antibodies were performed for each experiment. Fluorescence images were captured with a confocal microscope (Zeiss LSM 710).

**Aniline blue staining**

Aniline blue coloration was performed on ejaculated spermatozoa froms patients P0582 and fertile control. After washing twice with 5 ml of PBS 1×, a small portion of semen samples were fixed with a 3% glutaraldehyde solution in PBS 1× for 30 min at room temperature.

Slides were then incubated in a succession of baths: 5 min in water, 10 min in 5% aniline blue diluted in 4% acetic acid solution, twice for 2 min in water, 2 min in 70%, 90% and 100% ethanol solutions and finally for 2 min in toluene. Slides were then analyzed using a transmitted light microscope at 100× objective with oil. Dark blue cells were considered as positive, when lightly and very lightly stained cells were considered as negative.

**Hybridization *in situ* fluorescence**

FISH was performed on ejaculated spermatozoa from patients P0582 and fertile control. Sperm cells were prepared for hybridization like previously described[46]. Then, two spermFISH experiments were performed using a mix of 18 spectrum blue, X spectrum green and Y spectrum orange probes and a mix of 13 spectrum green and 21 spectrum orange probes. Scoring was performed with a device (METAFER Metasystems®) previously validated for spermFISH analysis[46] with additional verification of two trained users according to strict criteria[47].

## RESULTS

### Variant identification

Whole exome sequencing was performed on both azoospermic and teratozoospermic infertile men cohorts. In the azoospermia cohort, we identified two patients harboring bi-allelic pathogenic variants in *HENMT1* we previously flagged as candidate variants[33]. Patient P0109 carried a missense variant (c.226G>A;p.Gly76Arg) affecting an evolutionarily conserved glycine at position 76 (Figure 1A-B), while patient P0272 carried a truncating variant (c.456C>G;p.Tyr152Ter). In the teratozoospermia cohort, another individual (P0582) was discovered carrying a homozygous truncating c.100C>T;p.Gln34Ter variant in exon 2 of *HENMT1* (NM_001102592.2), and a second one (P1021) with the same variant as P0272 (c.456C>G;p.Tyr152Ter), findings corroborated by Sanger sequencing (Figure 1A).

We then performed a minigene assay to evaluate the deleterious impact of the p.Gly76Arg variant of P0109 and to characterize its effect on splicing. RT-PCR was conducted on RNA extracted from both non-transfected and transfected cells containing either the wild-type or mutant HENMT1 sequence in the minigene construct. In HEK cells transfected with the wild-type minigene, RT-PCR produced a 622 bp amplicon indicative of normal splicing (Figure S1C). In contrast, cells transfected with the mutant minigene generated a smaller 509 bp amplicon, which, upon Sanger sequencing, was found to contain exclusively exonic sequences from the vector, confirming aberrant splicing due to exon 4 skipping (Figure S1D).

The presence of spermatozoa in patient's ejaculate opens avenues for employing assisted reproduction technologies in their treatment.

**Patient characterization**

Patient P0582, a man of 43 years during the initial examination, sought consultation for infertility with his 27 years old wife at the Reproductive Biology laboratory-CECOS of Lille University Hospital (France). Patient P1021, a man of 37 years during the initial examination, sought consultation for infertility with his 34 years old wife at the Clinique des Jasmins of Tunis (Tunisia). Medical examinations of both wives revealed no apparent abnormalities. Both couples originated from Algeria and were born to unrelated parents. P1021 reported a family history of infertility, with paternal and maternal cousins affected. Physical examinations of both men revealed no abnormalities, and neither reported exposure to tobacco, drugs, medical treatments, or any reprotoxic environments. Three sperm analyses were conducted during their treatment, all diagnosing oligo-astheno-terato-necrozoospermia (Table 1). Spermocytogram revealed 100% of morphological abnormalities with a predominance of microzoospermic/pinhead, globocephalic/round and macrozoospermic/multiple sperm, along with flagellum abnormalities (Figure 1C). These findings were subsequently confirmed by TEM (Figure 1D), with no normal forms observed across all samples. Notably, many immature germ cells and isolated flagella were present in the ejaculate of both men (Table 1, Figure 1C).

**Patient care**

For P0582, three IVF-ICSI cycles resulted in the collection of 29 oocytes, 21 of which were injected. This led to the formation of 11 zygotes and the development of 10 embryos, of which eight were transferred. Despite achieving two biochemical pregnancies, no live births occurred (Table 2). For P1021, one IVF-ICSI attempt was conducted with the addition of calcium ionophore. Eleven oocytes were collected, eight were injected, resulting in four zygotes, all of which developed into embryos. This led to two embryo transfers, but no live birth occurred.

**Variant effect on protein**

*HENMT1* is located on chromosome 1 and contains eight exons encoding a predicted 393-amino acid protein (Q5T8I9). To demonstrate the influence of the candidate variant on protein expression and localization, we conducted immunofluorescence experiments using an anti-

HENMT1 antibody. The results displayed a strong signal in the neck and post-acrosomal region of fertile control sperm, accompanied by a faint signal along the entire flagellum. In contrast, no signal was detected in the patient's sperm cells, suggesting the absence or truncation of the protein (Figure 2). Due to the patients' phenotype, very few spermatozoa were available initially, and at this point, only a few spermatozoa from P0582 remained. The negative IVF-ICSI outcomes, along with prior observations of nuclear abnormalities in *Henmt1* knockout mice, prompted us to examine the nuclear quality of these scarce spermatozoa.

**Nuclear analysis**

Nuclear morphology was quantitatively assessed using Nuclear Morphology Analysis Software[48] (version 2.1, https://bitbucket.org/bmskinner/nuclear_morphology/wiki/Home), disclosing a notable enlargement and dysmorphia in P0582's sperm nucleus compared to the control sperm (Figure S2). Considering that this may be associated with aneuploidy, we conducted sperm fluorescent *in situ* hybridization (spermFISH) targeting chromosomes 13, 18, 21, X, and Y. The findings revealed a substantial rise in diploid sperm cells (16% compared to less than 1% in fertile controls) and an average aneuploidy increase of 2% across all examined chromosomes (Figure 3A). Extrapolation from these data suggests that the overall sperm aneuploidy for this patient could potentially reach up to 65%.

In the light of this result, we hypothesized that this condition might be associated with substantial DNA compaction defects. Subsequently, we conducted blue aniline coloration, which use the capacity of this acidic dye to binds to lysine residues to discriminate between lysine-rich histones and arginine- and cysteine-rich protamines[49-50]. All patient's sperm cells displayed a positive dark blue staining, indicating abnormal histone presence (Figure 3B).

## DISCUSSION

In the present work, we report two new patients harboring bi-allelic truncating variants in *HENMT1*, which results in extreme oligo-astheno-teratozoospermia phenotype. Our investigations revealed altered sperm concentration, mobility, morphology, nuclear DNA compaction and increased sperm aneuploidy. Multiple IVF-ICSI were conducted, yet no live births ensued despite two biological pregnancies.

The reproductive phenotypes associated with variants in piRNA biogenesis-related genes exhibit only partial overlap between mice and humans with notable phenotypic differences for some genes[11]. Most of the time, human spermatogenesis seems to allow further progression,

as seen in TDRD9 or FKBP6, where knockout mice exhibit meiotic arrest[21,32] while patients display severe oligozoospermia[11,32]. HENMT1 has been, until now, an exception to this pattern (as well as GPAT2[11,51], PIWIL2[52-53] and PLD6[54-55]) with Henmt1-knockout mice displaying an OAT phenotype[37] and patients displaying the more severe phenotype azoospermia[11,34]. We report here on two new patients with an OAT phenotype that is very similar to the one observed in mice, thus extending the phenotypic continuum of HENMT1 in men (see Table 3). It should be noted that while P1021's sperm morphology closely resembles the knockout mice one, characterized by a predominance of pinhead sperm and stumpy tails, P0582 exhibits a higher proportion of macrocephalic heads. Although both forms indicate altered spermatogenesis, this underscores once again the intricacy of the impairments resulting from piwi pathway alterations[34].

The origin of this continuum may lie in the nature of the different variants, which could affect the protein in various ways—from complete loss to truncation to a compromised version of the protein. Interestingly, the three patients with loss-of-function variants, which likely result in at least a severe truncation of the protein, exhibited a less severe phenotype than the patients with missense variants, where a less compromised protein is expected. This suggests that the complete absence of the protein might be less harmful than the presence of a malfunctioning protein. However, the clinical impact of genetics proves even more complex, as patients with the same p.Tyr152Ter variant exhibited phenotypes of varying severity. It is known that the same genetic variant can produce a spectrum of phenotypes in different individuals, ranging from no detectable clinical symptoms to severe disease, even among relatives[56]. These variants of variable expressivity, in which the same genotype can cause a wide range of clinical symptoms across a spectrum have already been reported in the context of male infertility[57]. This variability is believed to be driven by multiple factors, including common genetic variants, regulatory region variants, epigenetic modifications, environmental influences, and lifestyle[56].

Beyond the phenotype, the key question revolves around the potential for a therapeutic response in patients. Although the observed phenotypes fall short of the severity associated with azoospermia, it still presents a distinctive challenge. Indeed, the therapeutic approach for severe OAT phenotype involves IVF-ICSI, necessitating the selection of sperm with the most normal morphology possible. However, neither of the two patients exhibited any morphologically normal heads. Pinhead sperm, which possess minimal to no DNA content, and macrocephalic sperm which content excessive DNA, are both incompatible with successful pregnancies[58-60]. Given the impracticality of using these sperm for injection, the

operator has no choice but to utilize the remaining globocephalic spermatozoa (which explain the use of the artificial oocyte activation treatment during P1021 IVF-ICSI attempt). However, globozoospermic sperm have been associated with altered genome packaging, DNA damage and epigenetic modifications[61-63] compromising embryo development and successful pregnancy. The aneuploidy increase and the DNA compaction anomalies we reported here for P0582 underscore the need for future studies to investigate the presence of genetic and epigenetic anomalies in the sperm of HENMT1 variant carriers and their potential transmission to the offspring.

As of now, the medical counseling and management for carriers of HENMT1 variants appear to hold an unfavorable prognosis. No successful IVF treatments have been reported for these carriers, and concerns persist regarding the potential risk of transmission of genetic and epigenetics anomalies. Moreover, the variability observed among individuals emphasizes the need for caution in applying findings from one patient to another. A broader representation of carrier patients in the literature is required, as a successful pregnancy report would significantly shift the current pessimistic prognosis. Without additional case descriptions, it is also premature to extrapolate this unfavorable prognosis to all carriers of deleterious variants in piRNA biogenesis-related genes, despite the absence of documented successful pregnancies in carrier patients thus far.

In summary, further studies are required to establish guidelines for managing patients with mutations in HENMT1 or other piwi pathway genes. Nonetheless, our findings offer valuable initial insights to inform patients, despite the unfavorable prognosis.

**Acknowledgements**

We thank all patients and control individuals for their participation.

**Authors' roles**

Z.W., A-L.B., C.C. and G.M. analysed the data and wrote the manuscript; C.Ca., M.B., V.S., N.T-M., Z-E.K., F.P., C.C. and G.M. performed and analysed the genetic data; Z.W., E.F., J-P.H. an G.M. performed the sperm analysis and the IF experiments; A-L.B. and A.B. performed the electron microscopy experiments; A-L.B., P.P., S.F.B.M., R.Z. and Z-E.K. provided clinical samples and data; C.C. and G.M. designed the study, supervised all molecular laboratory work, had full access to all of the data in the study and took responsibility for the integrity of the data and its accuracy. All authors contributed to the report.

## Funding

This work was supported by the Institut National de la Santé et de la Recherche Médicale (INSERM), the Centre National de la Recherche Scientifique (CNRS), the University Grenoble Alpes, and the French National Research Agency (grant OLIGO-SPERM ANR-21-CE17-0007 to CC and GM; grant FLAGELOME ANR-19-CE17-0014 to PR).

## Conflict of interest

The authors declare no conflict of interest.

## REFERENCES

1. Datta J, Palmer MJ, Tanton C, et al. Prevalence of infertility and help seeking among 15 000 women and men. Hum Reprod. 2016;31(9):2108-2118. doi:10.1093/humrep/dew123

2. Sadeghi MR. Unexplained infertility, the controversial matter in management of infertile couples. J Reprod Infertil. 2015;16(1):1-2

3. Krausz C. Male infertility: pathogenesis and clinical diagnosis. Best Pract Res Clin Endocrinol Metab. 2011;25(2):271-285. doi:10.1016/j.beem.2010.08.006

4. Beurois J, Cazin C, Kherraf ZE, et al. Genetics of teratozoospermia: Back to the head. Best Pract Res Clin Endocrinol Metab. 2020;34(6):101473. doi:10.1016/j.beem.2020.101473

5. Tüttelmann F, Ruckert C, Röpke A. Disorders of spermatogenesis: Perspectives for novel genetic diagnostics after 20 years of unchanged routine. Med Genet. 2018;30(1):12-20. doi:10.1007/s11825-018-0181-7

6. Krausz C, Riera-Escamilla A. Genetics of male infertility. Nat Rev Urol. 2018;15(6):369-384. doi:10.1038/s41585-018-0003-3

7. Martinez G, Coutton C, Loeuillet C, et al. Oligogenic heterozygous inheritance of sperm abnormalities in mouse. Elife. 2022;11:e75373. Published 2022 Apr 22. doi:10.7554/eLife.75373

8. Du S, Li W, Zhang Y, et al. Cholesterol-Amino-Phosphate (CAP) Derived Lipid Nanoparticles for Delivery of Self-Amplifying RNA and Restoration of Spermatogenesis in Infertile Mice. Adv Sci (Weinh). 2023;10(11):e2300188. doi:10.1002/advs.202300188

9. Mann JM, Wei C, Chen C. How genetic defects in piRNA trimming contribute to male infertility. Andrology. 2023;11(5):911-917. doi:10.1111/andr.13324

10. Perillo G, Shibata K, Wu PH. piRNAs in sperm function and embryo viability. Reproduction. 2023;165(3):R91-R102. Published 2023 Jan 17. doi:10.1530/REP-22-0312

11. Stallmeyer B, Bühlmann C, Stakaitis R, et al. Inherited defects of piRNA biogenesis cause transposon de-repression, impaired spermatogenesis, and human male infertility. 2024, PREPRINT (Version 1). doi:10.21203/rs.3.rs-3710476/v1

12. Ozata DM, Gainetdinov I, Zoch A, O'Carroll D, Zamore PD. PIWI-interacting RNAs: small RNAs with big functions. Nat Rev Genet. 2019;20(2):89-108. doi:10.1038/s41576-018-0073-3

13. Wang J, Shi Y, Zhou H, et al. piRBase: integrating piRNA annotation in all aspects. Nucleic Acids Res. 2022;50(D1):D265-D272. doi:10.1093/nar/gkab1012

14. Wang X, Ramat A, Simonelig M, Liu MF. Emerging roles and functional mechanisms of PIWI-interacting RNAs [published correction appears in Nat Rev Mol Cell Biol. 2022 Nov;23(11):771. doi: 10.1038/s41580-022-00548-w]. Nat Rev Mol Cell Biol. 2023;24(2):123-141. doi:10.1038/s41580-022-00528-0

15. Kawase M, Ichiyanagi K. The Expression Dynamics of piRNAs Derived From Male Germline piRNA Clusters and Retrotransposons. Front Cell Dev Biol. 2022;10:868746. Published 2022 May 11. doi:10.3389/fcell.2022.868746

16. Loubalova Z, Konstantinidou P, Haase AD. Themes and variations on piRNA-guided transposon control. Mob DNA. 2023;14(1):10. Published 2023 Sep 2. doi:10.1186/s13100-023-00298-2

17. Özata DM, Yu T, Mou H, et al. Evolutionarily conserved pachytene piRNA loci are highly divergent among modern humans. Nat Ecol Evol. 2020;4(1):156-168. doi:10.1038/s41559-019-1065-1

18. Goh WS, Falciatori I, Tam OH, et al. piRNA-directed cleavage of meiotic transcripts regulates spermatogenesis. Genes Dev. 2015;29(10):1032-1044. doi:10.1101/gad.260455.115

19. Gou LT, Dai P, Yang JH, et al. Pachytene piRNAs instruct massive mRNA elimination during late spermiogenesis [published correction appears in Cell Res. 2015 Feb;25(2):266. doi: 10.1038/cr.2015.14]. Cell Res. 2014;24(6):680-700. doi:10.1038/cr.2014.41

20. Saxe JP, Chen M, Zhao H, Lin H. Tdrkh is essential for spermatogenesis and participates in primary piRNA biogenesis in the germline. EMBO J. 2013;32(13):1869-1885. doi:10.1038/emboj.2013.121

21. Shoji M, Tanaka T, Hosokawa M, et al. The TDRD9-MIWI2 complex is essential for piRNA-mediated retrotransposon silencing in the mouse male germline. Dev Cell. 2009;17(6):775-787. doi:10.1016/j.devcel.2009.10.012

22. Pandey RR, Tokuzawa Y, Yang Z, et al. Tudor domain containing 12 (TDRD12) is essential for secondary PIWI interacting RNA biogenesis in mice. Proc Natl Acad Sci U S A. 2013;110(41):16492-16497. doi:10.1073/pnas.1316316110

23. Bolcun-Filas E, Bannister LA, Barash A, et al. A-MYB (MYBL1) transcription factor is a master regulator of male meiosis. Development. 2011;138(15):3319-3330. doi:10.1242/dev.067645

24. Dong J, Wang X, Cao C, et al. UHRF1 suppresses retrotransposons and cooperates with PRMT5 and PIWI proteins in male germ cells. Nat Commun. 2019;10(1):4705. Published 2019 Oct 17. doi:10.1038/s41467-019-12455-4

25. Ichiyanagi T, Ichiyanagi K, Ogawa A, et al. HSP90α plays an important role in piRNA biogenesis and retrotransposon repression in mouse. Nucleic Acids Res. 2014;42(19):11903-11911. doi:10.1093/nar/gku881

26. Deng W, Lin H. miwi, a murine homolog of piwi, encodes a cytoplasmic protein essential for spermatogenesis. Dev Cell. 2002;2(6):819-830. doi:10.1016/s1534-5807(02)00165-x

27. Pan J, Goodheart M, Chuma S, Nakatsuji N, Page DC, Wang PJ. RNF17, a component of the mammalian germ cell nuage, is essential for spermiogenesis. Development. 2005;132(18):4029-4039. doi:10.1242/dev.02003

28. Zhou L, Canagarajah B, Zhao Y, et al. BTBD18 Regulates a Subset of piRNA-Generating Loci through Transcription Elongation in Mice. Dev Cell. 2017;40(5):453-466.e5. doi:10.1016/j.devcel.2017.02.007

29. Ghieh F, Barbotin AL, Swierkowski-Blanchard N, et al. Whole-exome sequencing in patients with maturation arrest: a potential additional diagnostic tool for prevention of recurrent negative testicular sperm extraction outcomes. Hum Reprod. 2022;37(6):1334-1350. doi:10.1093/humrep/deac057

30. Tan YQ, Tu C, Meng L, et al. Loss-of-function mutations in TDRD7 lead to a rare novel syndrome combining congenital cataract and nonobstructive azoospermia in humans. Genet Med. 2019;21(5):1209-1217. doi:10.1038/gim.2017.130

31. Arafat M, Har-Vardi I, Harlev A, et al. Mutation in TDRD9 causes non-obstructive azoospermia in infertile men. J Med Genet. 2017;54(9):633-639. doi:10.1136/jmedgenet-2017-104514

32. Wyrwoll MJ, Gaasbeek CM, Golubickaite I, et al. The piRNA-pathway factor FKBP6 is essential for spermatogenesis but dispensable for control of meiotic LINE-1 expression in humans. Am J Hum Genet. 2022;109(10):1850-1866. doi:10.1016/j.ajhg.2022.09.002

33. Wyrwoll MJ, van der Heijden GW, Krausz C, et al. Improved phenotypic classification of male infertility to promote discovery of genetic causes. *Nat Rev Urol*. 2024;21(2):91-101. doi:10.1038/s41585-023-00816-0

34. Kherraf ZE, Cazin C, Bouker A, et al. Whole-exome sequencing improves the diagnosis and care of men with non-obstructive azoospermia. Am J Hum Genet. 2022;109(3):508-517. doi:10.1016/j.ajhg.2022.01.011

35. Beyret E, Liu N, Lin H. piRNA biogenesis during adult spermatogenesis in mice is independent of the ping-pong mechanism. Cell Res. 2012;22(10):1429-1439. doi:10.1038/cr.2012.120

36. Czech B, Munafò M, Ciabrelli F, et al. piRNA-Guided Genome Defense: From Biogenesis to Silencing. Annu Rev Genet. 2018;52:131-157. doi:10.1146/annurev-genet-120417-031441

552 37. Lim SL, Qu ZP, Kortschak RD, et al. HENMT1 and piRNA Stability Are Required for
553 Adult Male Germ Cell Transposon Repression and to Define the Spermatogenic Program in
554 the Mouse [published correction appears in PLoS Genet. 2015 Dec;11(12):e1005782]. PLoS
555 Genet. 2015;11(10):e1005620. Published 2015 Oct 23. doi:10.1371/journal.pgen.1005620
556 38. Hempfling AL, Lim SL, Adelson DL, et al. Expression patterns of HENMT1 and PIWIL1
557 in human testis: implications for transposon expression. Reproduction. 2017;154(4):363-374.
558 doi:10.1530/REP-16-0586
559 39. Liang H, Jiao Z, Rong W, et al. 3'-Terminal 2'-O-methylation of lung cancer miR-21-5p
560 enhances its stability and association with Argonaute 2. Nucleic Acids Res.
561 2020;48(13):7027-7040. doi:10.1093/nar/gkaa504
562 40. Coutton C, Martinez G, Kherraf ZE, et al. Bi-allelic Mutations in ARMC2 Lead to Severe
563 Astheno-Teratozoospermia Due to Sperm Flagellum Malformations in Humans and Mice. Am
564 J Hum Genet. 2019;104(2):331-340. doi:10.1016/j.ajhg.2018.12.013
565 41. Martinez G, Beurois J, Dacheux D, et al. Biallelic variants in MAATS1 encoding
566 CFAP91, a calmodulin-associated and spoke-associated complex protein, cause severe
567 astheno-teratozoospermia and male infertility. J Med Genet. 2020;57(10):708-716.
568 doi:10.1136/jmedgenet-2019-106775
569 42. McLaren W, Gil L, Hunt SE, et al. The Ensembl Variant Effect Predictor. Genome Biol.
570 2016;17(1):122. Published 2016 Jun 6. doi:10.1186/s13059-016-0974-4
571 43. Roux-Buisson N, Rendu J, Denjoy I, et al. Functional analysis reveals splicing mutations
572 of the CASQ2 gene in patients with CPVT: implication for genetic counselling and clinical
573 management. Hum Mutat. 2011;32(9):995-999. doi:10.1002/humu.21537
574 44. World Health Organization, WHO laboratory manual for the examination and processing
575 of human semen. 6th ed. 2021, Geneva: World Health Organization.
576 45. Boursier A, Boudry A, Mitchell V, et al. Results and perinatal outcomes from 189 ICSI
577 cycles of couples with asthenozoospermic men and flagellar defects assessed by transmission
578 electron microscopy. Reprod Biomed Online. 2023;47(5):103328.
579 doi:10.1016/j.rbmo.2023.103328
580 46. Martinez G, Gillois P, Le Mitouard M, et al. FISH and tips: a large scale analysis of
581 automated versus manual scoring for sperm aneuploidy detection. Basic Clin Androl.
582 2013;23:13. Published 2013 Dec 1. doi:10.1186/2051-4190-23-13
583 47. Guyot C, Gandula M, Noordermeer W, et al. FISH and Chimps: Insights into Frequency
584 and Distribution of Sperm Aneuploidy in Chimpanzees (Pan troglodytes). Int J Mol Sci.
585 2021;22(19):10383. Published 2021 Sep 27. doi:10.3390/ijms221910383

48. Skinner BM, Rathje CC, Bacon J, et al. A high-throughput method for unbiased quantitation and categorization of nuclear morphology†. Biol Reprod. 2019;100(5):1250-1260. doi:10.1093/biolre/ioz013

49. Hofmann N, Hilscher B. Use of aniline blue to assess chromatin condensation in morphologically normal spermatozoa in normal and infertile men. Hum Reprod. 1991;6(7):979-982. doi:10.1093/oxfordjournals.humrep.a137472

50. Gusse M, Sautière P, Bélaiche D, et al. Purification and characterization of nuclear basic proteins of human sperm. Biochim Biophys Acta. 1986;884(1):124-134. doi:10.1016/0304-4165(86)90235-7

51. Shiromoto Y, Kuramochi-Miyagawa S, Nagamori I, et al. GPAT2 is required for piRNA biogenesis, transposon silencing, and maintenance of spermatogonia in mice†. Biol Reprod. 2019;101(1):248-256. doi:10.1093/biolre/ioz056

52. Kuramochi-Miyagawa S, Kimura T, Ijiri TW, et al. Mili, a mammalian member of piwi family gene, is essential for spermatogenesis. Development. 2004;131(4):839-849. doi:10.1242/dev.00973

53. Alhathal N, Maddirevula S, Coskun S, et al. A genomics approach to male infertility. Genet Med. 2020;22(12):1967-1975. doi:10.1038/s41436-020-0916-0

54. Watanabe T, Chuma S, Yamamoto Y, et al. MITOPLD is a mitochondrial protein essential for nuage formation and piRNA biogenesis in the mouse germline. Dev Cell. 2011;20(3):364-375. doi:10.1016/j.devcel.2011.01.005

55. Nagirnaja L, Lopes AM, Charng WL, et al. Diverse monogenic subforms of human spermatogenic failure. Nat Commun. 2022;13(1):7953. Published 2022 Dec 26. doi:10.1038/s41467-022-35661-z

56. Kingdom R, Wright CF. Incomplete Penetrance and Variable Expressivity: From Clinical Studies to Population Cohorts. *Front Genet*. 2022;13:920390. Published 2022 Jul 25. doi:10.3389/fgene.2022.920390

57. Kherraf ZE, Cazin C, Lestrade F, et al. From azoospermia to macrozoospermia, a phenotypic continuum due to mutations in the ZMYND15 gene. Asian J Androl. 2022;24(3):243-247. doi:10.4103/aja202194

58. Ghédir H, Gribaa M, Mamaî O, et al. Macrozoospermia: screening for the homozygous c.144delC mutation in AURKC gene in infertile men and estimation of its heterozygosity frequency in the Tunisian population. J Assist Reprod Genet. 2015;32(11):1651-1658. doi:10.1007/s10815-015-0565-4

59. Agarwal A, Sharma R, Gupta S, et al. Sperm Morphology Assessment in the Era of Intracytoplasmic Sperm Injection: Reliable Results Require Focus on Standardization, Quality Control, and Training. World J Mens Health. 2022;40(3):347-360. doi:10.5534/wjmh.210054

60. Ounis L, Zoghmar A, Coutton C, et al. Mutations of the aurora kinase C gene causing macrozoospermia are the most frequent genetic cause of male infertility in Algerian men. Asian J Androl. 2015;17(1):68-73. doi:10.4103/1008-682X.136441

61. Yassine S, Escoffier J, Martinez G, et al. Dpy19l2-deficient globozoospermic sperm display altered genome packaging and DNA damage that compromises the initiation of embryo development. Mol Hum Reprod. 2015;21(2):169-185. doi:10.1093/molehr/gau099

62. Wang XX, Sun BF, Jiao J, et al. Genome-wide 5-hydroxymethylcytosine modification pattern is a novel epigenetic feature of globozoospermia. Oncotarget. 2015;6(9):6535-6543. doi:10.18632/oncotarget.3163

63. Beurois J, Cazin C, Kherraf ZE, et al. Genetics of teratozoospermia: Back to the head. Best Pract Res Clin Endocrinol Metab. 2020;34(6):101473. doi:10.1016/j.beem.2020.101473

## Figure legends

Figure 1. (A) Electropherograms from Sanger sequencing indicating the presence of the c.100C>T variant in patient P0582 and c.456C>G variant (NM) in patient P1021 (NM_001102592.2), as well as the two previously identified variants c.226G>A and c.456C>G in patients P0109 and P0272, respectively. The positions of these observed variants are indicated on the structure of the canonical transcript of *HENMT1*, and their impact on the HENMT1 protein is visually represented using modeling from SWISS-MODEL for the truncated and mutated proteins. (B) Conservation and alignment of *HENMT1* sequences from various orthologs surrounding the missense variant identified in the patient P0109. (C) Light microscopy analysis of spermatozoa obtained from a fertile control individual and patient P0582. All spermatozoa from patient P0582 exhibited abnormal morphology, including macrocephalic multi-flagellated sperm (white arrow), globozoospermic sperm (black arrow) and pinhead sperm (blue arrow) along numerous immature germ cells (far right panel). Scale bar = 10 µm. (D) Transmission electron microscopy analysis of sperm cells from patient P0582, revealing abnormal sperm with multiple abnormal nuclei.

Figure 2. HENMT1 immunostaining of sperm cells obtained from a fertile control individual and patient P0582 with the c.100C>T variant. Sperm cells were subjected to labeling using an anti-HENMT1 antibody (red), an anti-acetylated tubulin antibody (green), and DAPI (blue) for nuclear staining. In the fertile control, the HENMT1 signal was detected with high intensity at the neck and post-acrosomal region of sperm heads, and a discrete signal throughout the entire length of the flagellum. Conversely, in all sperm from patient P0582, regardless of their morphology, the HENMT1 signal was completely absent. No antibody signals were detected in the negative control. Scale bars: 10 µm.

Figure 3. (A) spermFISH analysis of P0582 spermatozoa using a mix of 18 spectrum blue, X spectrum green and Y spectrum orange probes and a mix of 13 spectrum green and 21 spectrum orange probes. Histograms display the results for each experiment (left) and some illustrations are presented (right). (B) Control and patient P0582 spermatozoa were stained with aniline blue. In contrast to the control, all of the patient's sperm exhibited a strong blue staining.

Figure S1. Minigene Splicing Reporter Assay for HENMT1 Exon 4. (A) Amplification Strategy for HENMT1 Exon 4. The genomic HENMT1 sequence encompassing exon 4 was amplified, including flanking intronic regions, to facilitate splicing analysis. (B) Insertion Strategy into the pCineo Minigene Vector. HENMT1 exon 4 was inserted into the pCineo minigene vector in place of exon 9 of the CASQ2 gene. This replacement allows assessment of exon 4 splicing within the minigene construct. (C) RT-PCR Gel Electrophoresis. Results of RT-PCR show a smaller band in cells transfected with the mutated minigene compared to the control, indicating a splicing alteration. (D) Sanger Sequencing of RT-PCR Products. Chromatogram from Sanger sequencing confirms in HENMT1_exon 4 skipping, as demonstrated by the direct junction of CASQ2 exons 8 and 10 in cells transfected with the mutated minigene.

Figure S2. Nuclear morphology analysis of control (blue) and P0582 (yellow) sperm head obtained thanks to the Nuclear morphology software (version 1.19.2, https://bitbucket.org/bmskinner/nuclear_morphology/wiki/Home), according to the analysis method described in Skinner et al., 2019 (doi:10.1093/biolre/ioz013). Consensus nuclear outlines (left panel) and angle profiles (bottom) of control and patient P0582. The x axis represents an index of the percentage of the total perimeter as measured counterclockwise from the apex of the sperm nucleus and the y axis represents the interior angle measured across a sliding window centered on each index location. Statistical significance of differences between populations were assessed by the software, applying a Mann-Whitney U test with Bonferroni multiple testing correction. p-values were considered significant when inferior to 0.05.

694
695
696
697
698
699
700
701
702
703
704
705
706
707
708
709
710
711
712
713
714
715

## TABLES

**Table 1. Detailed semen parameters of patients P0582 and P1021.**

| | P0582 | | | P1021 | | | Normal range |
|---|---|---|---|---|---|---|---|
| **Date** | **17/09/2018** | **20/11/2018** | **18/11/2020** | **30/01/2023** | **08/07/2023** | **14/07/2023** | |
| **Specimen characteristics** | | | | | | | |
| Abstinence duration (days) | 3 | 3 | 4 | 4 | 7 | 4 | 2-7 |
| Volume (mL) | 4,5 | 0,87 | 5,1 | 3 | 5 | 1,2 | >1,5 |
| pH | 7,9 | 8,1 | 7,9 | na | na | na | >7,2 |
| Viscosity | weak | weak | normal | normal | normal | normal | |
| **Numeration** | | | | | | | |
| Sperm count ($10^{\wedge 6}$/ml) | 0,3 | 0,185 | 0,8 | 0,14 | 0,2 | 0,2 | >15 |
| Total numeration ($10^{\wedge 6}$/ejaculate) | 1,35 | 0,161 | 4,08 | 0,42 | 1 | 0,24 | >39 |
| Round cells ($10^{\wedge 6}$/ml) | 2,65 | 2,1 | 1,9 | 0,28 | 0,66 | na | <5 |
| Polynuclear ($10^{\wedge 6}$/ml) | 1,64 | 0,42 | 0,67 | na | na | na | <1 |
| **Motility** | | | | | | | |
| Progressive sperm (%) | 0 | 0 | 0 | 0 | 1 | 0 | >32 |
| Non progressive sperm (%) | 0 | 0 | 0 | 0 | 1 | 0 | P+NP>40 |
| Immotile sperm (%) | 100 | 100 | 100 | 100 | 99 | 100 | <60 |
| **Other tests** | | | | | | | |
| Vitality (% alive) | 10 | 10 | 26 | 0 | 5 | 4 | >58 |
| **Morphology** | | | | | | | |
| Normal (%) | 0 | 0 | 0 | 0 | 0 | 0 | >4 |
| Abnormal (%) | 100 | 100 | 100 | 100 | 100 | 100 | <96 |
| Head anomaly (%) | na | na | 100 | 100 | 100 | na | |
| *Elongated (%)* | *na* | *na* | *5* | *4* | *0* | *na* | |
| *Thinned (%)* | *na* | *na* | *0* | *0* | *0* | *na* | |
| *Microcephalic/Pinhead (%)* | *na* | *na* | *19* | *64* | *70* | *na* | |
| *Globocephalic/Round (%)* | *na* | *na* | *34* | *40* | *50* | *na* | |
| *Macrocephalic/Multiple (%)* | *na* | *na* | *47* | *16* | *20* | *na* | |
| *Abnormal base (%)* | *na* | *na* | *65* | *36* | *48* | *na* | |
| *Malformed acrosome (%)* | *na* | *na* | *100* | *100* | *100* | *na* | |
| Intermediate piece anomaly (%) | na | na | 38 | 28 | 34 | na | |
| *Cytoplasmic residue (%)* | *na* | *na* | *11* | *4* | *8* | *na* | |
| *Thin (%)* | *na* | *na* | *0* | *0* | *0* | *na* | |
| *Angulation (%)* | *na* | *na* | *28* | *24* | *26* | *na* | |
| Flagellum anomaly (%) | na | na | 95 | 74 | 92 | na | |
| *Absent (%)* | *na* | *na* | *5* | *0* | *0* | *na* | |

| | | | | | | |
|---|---|---|---|---|---|---|
| *Short (%)* | *na* | *na* | *13* | *4* | *16* | *na* |
| *Irregular size (%)* | *na* | *na* | *47* | *48* | *64* | *na* |
| *Coiled (%)* | *na* | *na* | *7* | *0* | *2* | *na* |
| *Multiple (%)* | *na* | *na* | *23* | *22* | *10* | *na* |

**Table 2. ICSI outcomes with sperm cells from the patient P0582 and P121.**

| **IVF-ICSI** | **P0582 n°1** | **P0582 n°2** | **P0582 n°3** | **P1021 n°1** |
|---|---|---|---|---|
| Date | 10/2019 | 05/2021 | 11/2022 | 07/2023 |
| Use of calcium ionophore | No | No | No | Yes |
| Collected oocytes | 14 | 11 | 4 | 11 |
| Injected oocytes | 8 | 10 | 3 | 8 |
| Zygotes | 3 | 6 | 2 | 4 |
| Unfertilised | 4 | 4 | 1 | 3 |
| Lysed | 1 | 0 | 0 | 1 |
| Day-2/3 embryos | 3 | 6 | 1 | 4 |
| Day-2/3 embryos with <10% fragmentation and expected cell stage | 1 | 2* | 0 | 2 |
| Transfers at D2 or D3 (fresh or frozen) | 3 | 2 | 0 | 2 |
| Transfer at blastocyst stage (fresh or frozen) | 0 | 2 | 1** | 0 |
| Biochemical pregnancy | 0 | 1 | 1 | 0 |
| Ultrasound pregnancy | 0 | 0 | 0 | 0 |
| Childbirth | 0 | 0 | 0 | 0 |

* of the four supernumerary that were kept in culture until Day-6 because they exhibited 4 cell on Day 3, two embryos evolved until the blastocyst stage, graded B4BB according to gardner's classification (Gardner and Schoolcraft, 1999). The two blastocysts were frozen for subsequent embryo transfer. ** the embryo was transferred at the morula compacted stage at Day-5

**Table 3. Patients' summary.**

| Patient | Variant | Consequence | Exon | Phenotype | Testis sperm retrieval | Childbirth | Reference |
|---|---|---|---|---|---|---|---|
| P0582 | c.100C>T; p.Gln34Ter | stop gained | 2/7 | Severe OAT | - | No | This study |
| P0109 | c.226G>A; p.Gly76Arg | missense | 3/7 | Azoospermia (MeA) | Negative | No | Kherraf et al., 2022 |
| M3079 | c.400A>T ; p.Ile134Leu | missense | 5/7 | Azoospermia (RsA) | Negative | No | Stallmeyer et al., 2024 |
| P0272 | c.456C>G; p.Tyr152Ter | stop gained | 5/7 | Azoospermia (Hypo) | Positive | No | Kherraf et al., 2022 |
| P1021 | c.456C>G; p.Tyr152Ter | stop gained | 5/7 | Severe OAT | - | No | This study |

MeA : Meiotic arrest ; RsA : Round spermatid arrest ; Hypo : Hypospermatogenesis ; OAT : Oligo-astheno-teratozoospermia

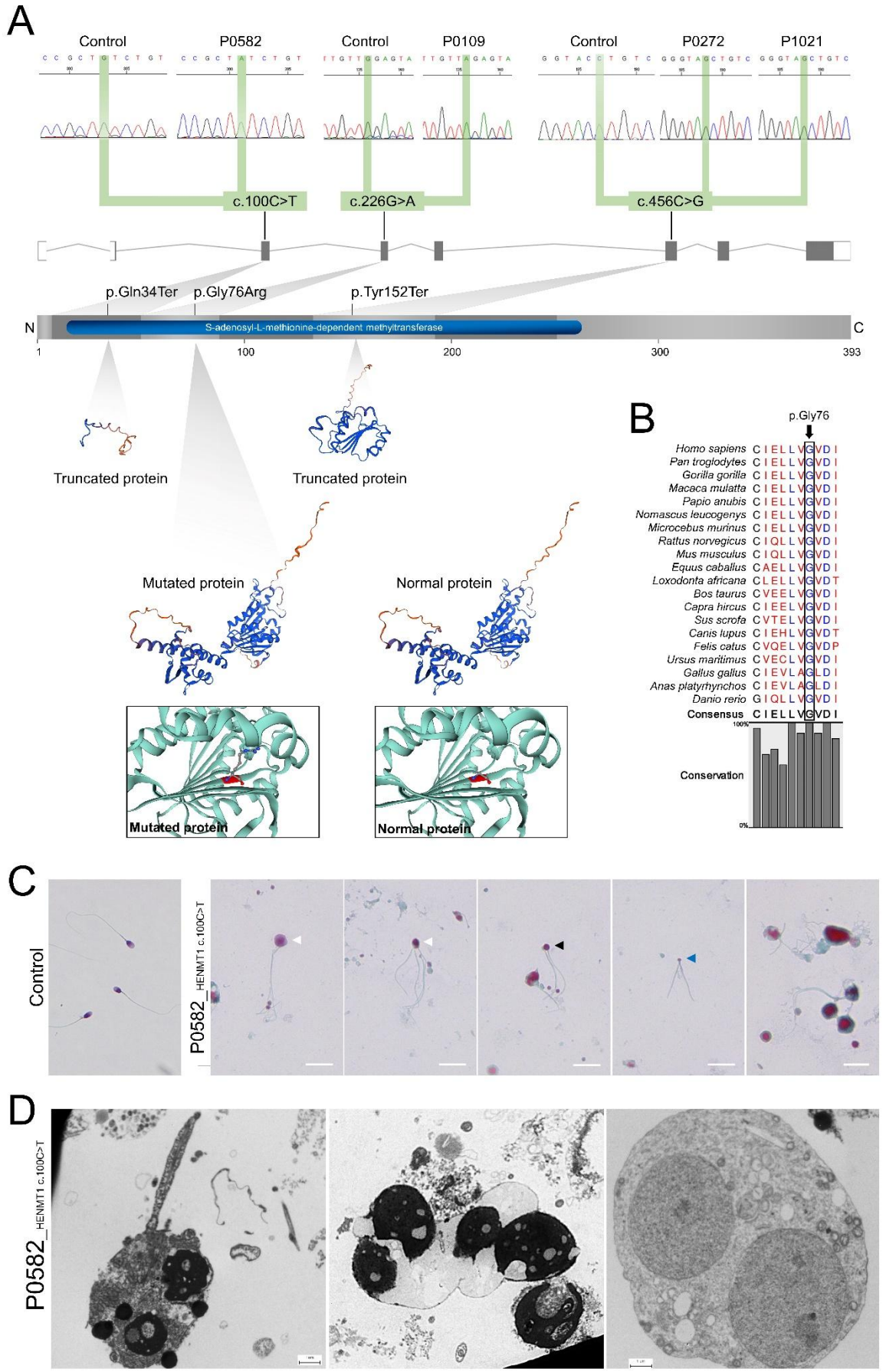
A
Control
P0582
Control
P0109
Control
P0272
P1021
c.100C>T
c.226G>A
c.456C>G
p.Gln34Ter
p.Gly76Arg
p.Tyr152Ter
N
S-adenosyl-L-methionine-dependent methyltransferase
C
1
100
200
300
393
Truncated protein
Truncated protein
Mutated protein
Normal protein
Mutated protein
Normal protein
B
p.Gly76
Homo sapiens C I E L L V G V D I
Pan troglodytes C I E L L V G V D I
Gorilla gorilla C I E L L V G V D I
Macaca mulatta C I E L L V G V D I
Papio anubis C I E L L V G V D I
Nomascus leucogenys C I E L L V G V D I
Microcebus murinus C I E L L V G V D I
Rattus norvegicus C I Q L L V G V D I
Mus musculus C I Q L L V G V D I
Equus caballus C A E L L V G V D I
Loxodonta africana C L E L L V G V D T
Bos taurus C V E E L V G V D I
Capra hircus C I E E L V G V D I
Sus scrofa C V T E L V G V D I
Canis lupus C I E H L V G V D T
Felis catus C V Q E L V G V D P
Ursus maritimus C V E C L V G V D I
Gallus gallus C I E V L A G L D I
Anas platyrhynchos C I E V L A G L D I
Danio rerio G I Q L L V G V D I
Consensus C I E L L V G V D I
100%
Conservation
0%
C
Control
P0582_HENMT1 c.100C>T
D
P0582_HENMT1 c.100C>T

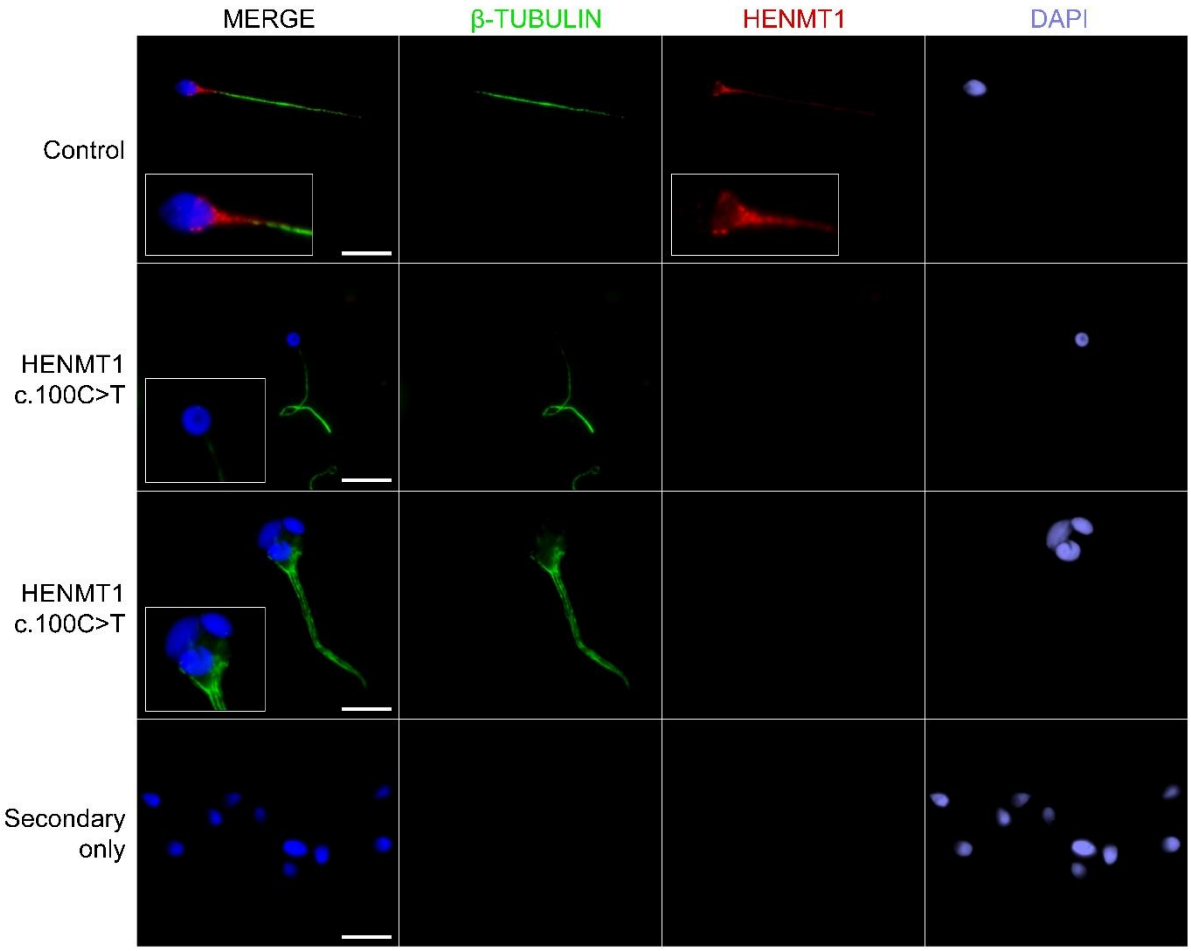
MERGE
β-TUBULIN
HENMT1
DAPI
Control
HENMT1 c.100C>T
HENMT1 c.100C>T
Secondary only

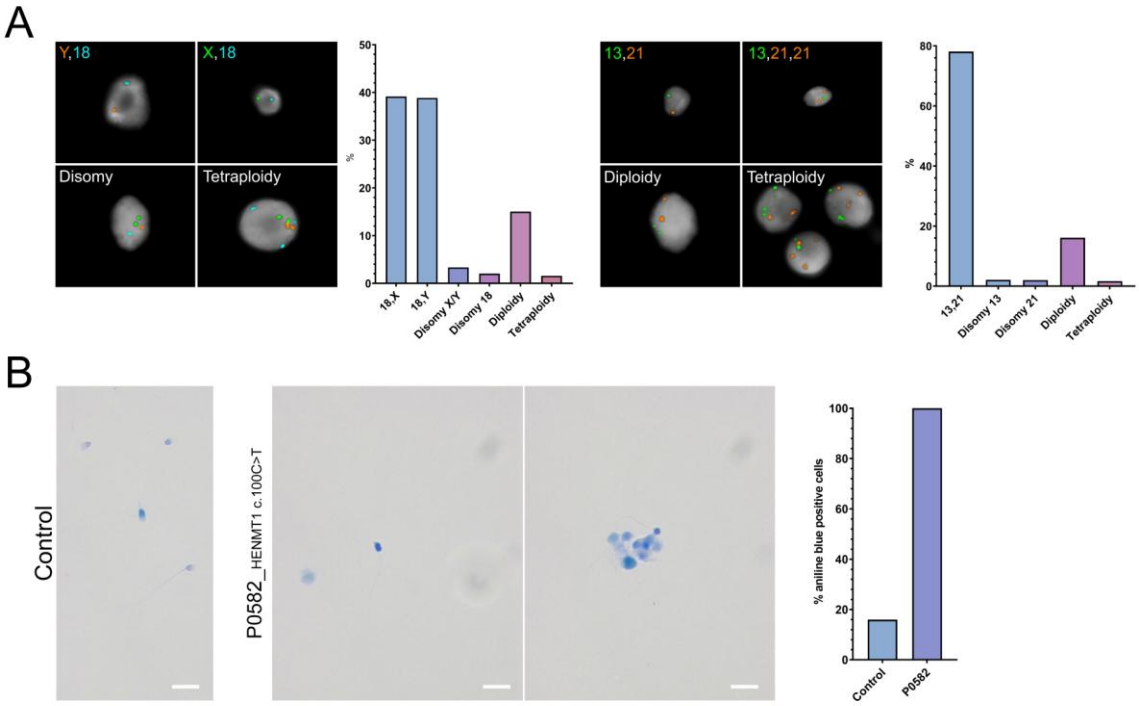
A
Y,18
X,18
Disomy
Tetraploidy
%
18,X
18,Y
Disomy X/Y
Disomy 18
Diploidy
Tetraploidy
13,21
13,21,21
Diploidy
Tetraploidy
%
13,21
Disomy 13
Disomy 21
Diploidy
Tetraploidy
B
Control
P0582_HENMT1 c.100C>T
% aniline blue positive cells
Control
P0582

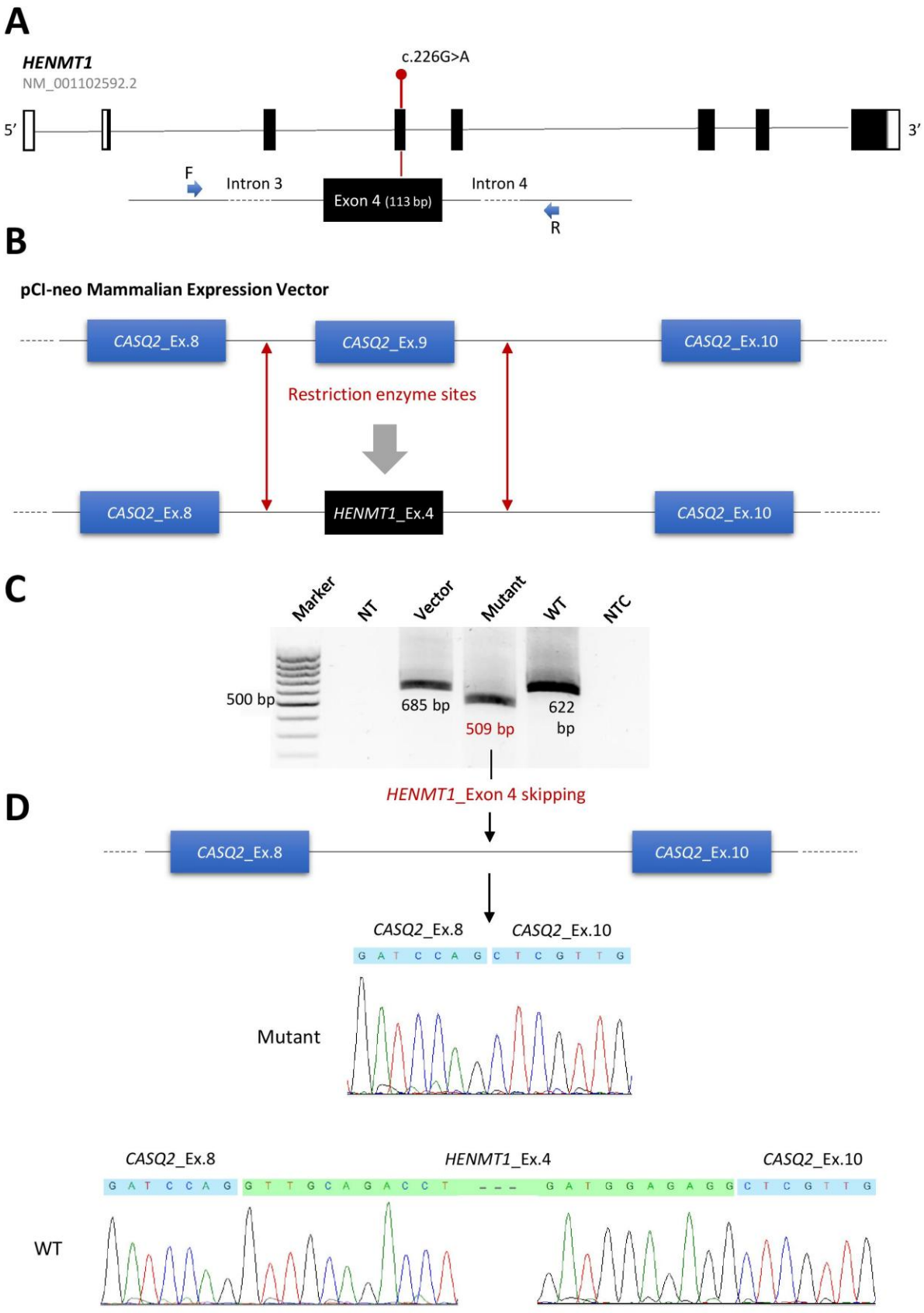
A
HENMT1
NM_001102592.2
c.226G>A
5′
3′
F
Intron 3
Exon 4 (113 bp)
Intron 4
R
B
pCI-neo Mammalian Expression Vector
CASQ2_Ex.8
CASQ2_Ex.9
CASQ2_Ex.10
Restriction enzyme sites
CASQ2_Ex.8
HENMT1_Ex.4
CASQ2_Ex.10
C
Marker
NT
Vector
Mutant
WT
NTC
500 bp
685 bp
509 bp
622 bp
HENMT1_Exon 4 skipping
D
CASQ2_Ex.8
CASQ2_Ex.10
CASQ2_Ex.8
CASQ2_Ex.10
G A T C C A G C T C G T T G
Mutant
CASQ2_Ex.8
HENMT1_Ex.4
CASQ2_Ex.10
G A T C C A G G T T G C A G A C C T G A T G G A G A G G C T C G T T G
WT

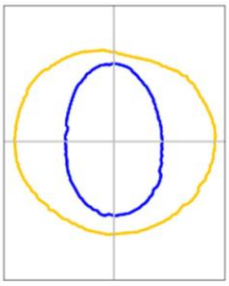

| Parameters | Control | Patient | Statistical values |
|---|---|---|---|
| Area 95% CI (µm²) | 66,40 ± 0,63 | 3186,83 ± 104,78 | >0,0001 |
| Perimeter 95% CI (µm²) | 31,95 ± 0,18 | 57,02 ± 5,15 | >0,0001 |
| Max feret mean 95% CI | 11,87 ± 0,08 | 18,66 ± 1,68 | >0,0001 |
| Circularity 95% CI | 0,81 | 0,87 | >0,0001 |
| Min diameter 95% CI (µm) | 7,14 ± 0,04 | 15,11 ± 1,23 | >0,0001 |
| Ellipticity 95% CI | 0,66 ± 0,01 | 0,97 ± 0,03 | >0,0001 |
| Aspect ratio 95% CI | 1,56 ± 0,01 | 1,05 ± 0,03 | >0,0001 |
| Elongation 95% CI | 0,21 ± 0,01 | 0,02 ± 0,01 | >0,0001 |